International Journal of Engineering Research & Technology (IJERT)
ISSN: 2278-0181
Vol. 3 Issue 9, September- 2014

Optical, Structural and Catalytic Evaluation of Gamma-Irradiation Synthesized Ag/PVA Nanocomposite Films

Z. I. Ali, H. H. Saleh And T. A. Afify
National Center for Radiation Research and Technology,
Radiation Chemistry Department,
P.O. Box 29 Nasr City, Cairo,
Atomic Energy Authority (AEA), Egypt

Abstract :- **Optical, structural and catalytic properties of silver/poly (vinyl alcohol) (Ag/PVA) nanocomposites were investigated as a function of gamma irradiation dose. A blue shift was observed in the UV/VIS absorption peak of PVA doped with silver nanoparticles (AgNPs) with increasing irradiation dose. However, a red shift was observed with increased Ag^+ ion molar concentration. The intensity, sharpness and symmetry of the surface plasmon resonance peak increases with increasing either irradiation dose or $AgNO_3$ molar concentration. The X-ray diffraction patterns showed the formation of the $AgNP_S$ in face cubic structure with different sizes as a function of either irradiation dose or Ag^+ ion molar concentrations. The catalytic evaluation of the investigated samples indicated active reduction of aromatic nitro compound with respect to the corresponding amino derivatives. The rate constant for reduction reaction of 4-nitrophenol (4-NP) into 4-aminophenol (4-AP) using Ag/PVA nanocomposite films was found to increase with increasing Ag molar concentration and irradiation dose. In conclusion, this procedure is simple and useful for large scale synthesis.**

Key words: Gamma-irradiation; Poly (vinyl alcohol); Ag nanoparticles; UV/VIS; XRD; Catalytic properties.

I. INTRODUCTION

The advantage of gamma-radiation induced synthesis of Ag nanoparticles lies in the fact that the desired highly reducing radicals can be generated without formation of any byproduct. When $AgNO_3$ precursor is embedded into PVA matrix, the optical properties are the net result of the electronic transition of the two components. Polymers have been frequently used as particle stabilizer and capping agent in radiation synthesis of metal nanoparticles, since they prevent agglomeration and precipitation of the nanoparticles. The embedding of such nanoparticles in polymer matrix is also advantageous from the point of view of film casting. The polymer films having nanoparticles in it can be considered as potential candidates for their use in electronic and optoelectronic devices. One of the major requirements of course, is being the observation of desired optical or electrical properties. Poly (vinyl alcohol) is known to be a good stabilizer of metal nanoparticles. Also, PVA is indeed well known for its wide range of potential applications in optical, pharmaceutical, medical, and membrane fields. Moreover, it is a water-soluble polymer and allows the development of environment-friendly material processes. Finally, it can react with metal salts via formation of chelate with metal cations in an aqueous solution and also act as a capping agent **[1]**.

The optical properties of metal nanoparticles are caused by collective oscillation of free and conducting electrons and metallic surface that interact with electromagnetic radiation. Surface plasmon resonance peaks (SPRP), appearing in the visible region for Ag/PVA nanocomposite films are characteristic of the noble metal nanoparticles. The electric field induces the dipole formation in the nanoparticles. A restoring force in the particle tries to compensate for this, resulting in a unique resonance wavelength **[2]**. Localized surface plasmons (LSPs) are charge density oscillations confined to metallic nanoparticles (sometimes referred to as metal clusters) and metallic nanostructures. Excitation of LSPs by an eclectic field (light), at an incident wavelength where resonance occur result in strong light scattering, in the presence of intense surface plasmon (SP) absorption bands, and an enhancement of the local electromagnetic fields. The frequency (i.e., absorption maxima or color) and intensity of the SP absorption bands are characteristics of the type of material (typically, gold, silver or platinum) and are highly sensitive to the size, size distribution and shape of the nanostructures, as well as to the environments which surround them. These are the precise properties which have promoted the ongoing intense interesting LSPs and fueled the construction of LSP-based sensors and devises in ever increasing variety. The intense yellowish brown color of aqueous dispersion colloidal of silver particles is of course, a manifestation of localized surface plasmon resonance **[3].** The present work is undertaken to study the optical, structural and catalytic properties of silver/poly (vinyl alcohol) (Ag/PVA) nanocomposites as a function of gamma irradiation dose.

II. EXPERIMENTAL

2.1. Materials

Silver nitrate ($AgNO_3$) was purchased from Nice Chemicals PVT, LTD Cochin-682024, India, poly (vinyl alcohol) (PVA), M.wt. = 32.000 were obtained from El-Goumhouria Co., Egypt. Sodium borohydride ($NaHB_4$) was purchased from Win lab,

2.2. Preparation of Ag/PVA nanocomposites

PVA solution was first prepared by dissolving 6 gm in 100 ml distilled water, then warmed up to ~60^{o}C and thoroughly stirred for 4h until the polymer became completely soluble. $AgNO_3$ solutions with different molar concentrations (from 0.005 up to 0.1 M), were added to the PVA solutions with continuous stirring for 2 h at 60^{o}C to allow silver ions to chelate into PVA chain. The Ag/PVA solutions were then left to cool at room temperature before adjusting the pH of the solution at 3 using diluted nitric acid (0.1 M). Finally, the Ag/PVA matrix was cast on a Petri dish. Homogenous Ag/PVA films were obtained after drying at room temperature for 48 h in order to remove residual distilled water. The Ag/PVA films were gamma irradiated at different doses (25-100 kGy) using Gamma cell 220 Excel ^{60}Co irradiation facility installed at the National Center for Radiation Research and Technology, NCRRT, Nasr City, Cairo, Egypt (manufactured by the Atomic Energy Authority of India).

2.3. Characterization techniques

2.3.1. UV/VIS spectroscopy

UV double beam ultraviolet/visible (UV/VIS) (Unicam spectrometer made in England), was used for scanning the absorption spectra in the range from 190 nm to 1000 nm wavelengths and measuring the optical density at λ_{max} for unirradiated and irradiated nanocomposite films.

2.3.2. X-ray diffraction (XRD) measurements

X-ray diffraction (XRD) patterns of the investigated films were determined by X-ray diffractometer (a Shimadzu XRD 600). XRD patterns in the θ range between 2θ of 4° to 90° were obtained at a scan rate of 2° /min on the diffractometer with CuK radiation source, a generator voltage of 40 KV, a generator current of 40 mA and a wavelength of 0.1546 nm at room temperature. All the diffraction patterns were examined at room temperature and under constant operation conditions.

2.3.3. Catalytic study of Ag/PVA nanocomposite films

In a typical experiment, 0.0189 g of $NaBH_4$ was added to 10 ml of 4-nitrophenol aqueous solution (0.00005 M) under stirring. A square piece sample of Ag/PVA nanocomposite film (0.9 cm side length) containing 0.05 M of $AgNO_3$ and gamma-irradiated at 75 kGy was placed at the bottom of quartz cuvette of path length 1 cm. Thereafter, 3 ml of the 4-nitrophenol solution were transferred to the cuvette. The degradation of 4-nitrophenol to 4-aminophenol was monitored by measuring the absorption peak at 400 nm recorded by the successive UV/VIS spectra.

III. RESULTS AND DISCCUSION

3.1. UV/VIS spectroscopy of Ag/PVA nanocomposite films

Fig. 1-2 show the UV/VIS absorption spectra of unirradiated and irradiated Ag/PVA nanocomposite films. Unirradiated Ag/PVA films did not exhibit any absorption peak in the entire UV/VIS range. **As shown in Fig.1**, the surface plasmon resonance absorption peak at 422 nm for irradiated Ag/PVA nanocomposite film (Ag (0.005M) was increased with increasing irradiation dose up to 75 kGy indicating the formation of silver nanoparticles. The increase of surface plasmon resonance intensity with increasing irradiation dose indicates the increase of silver nanoparticle content i.e. more reduction of Ag^+ to Ag nanoparticles. The decrease in the intensity of this band at higher irradiation dose (100 kGy) may be understood as follows: at higher irradiation doses, gamma irradiation induces chain scissions in the polymer matrix. Thus, the polymer chains acquired mobility along with the time of experiment scale. As the polymer chains relax, stresses are released. This causes Ag nanoparticles to move again; allowing crystals to aggregate and/or agglomerate which in turn reduces the absorption band intensity and increases λ_{max} absorption wavelength (red shift). It is well known that, the surface plasmon resonance peak of metal nanoparticles is sensitive to their surrounding environment absorption of the electrons in the conduction band of silver **[1, 4].** It was noticed that the intensity, order, sharpens, and symmetry of the observed surface plasmon resonance peak for samples containing higher $AgNO_3$ molar concentration, i.e. Ag nanoparticles are more pronounced and increases with increasing irradiation dose (see Fig. 2). In other words, the surface plasmon resonance peak gets narrower and sharper and also gradually increases in the intensity with increasing either irradiation dose or Ag nanoparticles. The predominate peak in the visible region at about 415-425 nm is attributed to the surface plasmon resonance nature of free electrons in the conduction bands of Ag nanoparticles, embedded in a dielectric medium. The symmetric shape of the surface plasmon resonance peak features the spherical shape and uniform distribution of Ag nanoparticles within the PVA matrix. Similar results were observed by several authors **[1].**

As the irradiation dose increased (25 to 75 kGy), the surface plasmon resonance peak is shifted from 422 to 414 nm indicating the presence of blue shift and the occurrence of quantum size effect, (i.e. formation of smaller metal nanoparticles), **[5].** The particle size is probably related to either the irradiation dose or the amount of the stabilizing polymer's chains. With increasing irradiation dose, the individual macromolecules of PVA are assumed to be crosslinked, giving rise to a three dimensional network. The crosslinking of polymer molecules results in a significant increase in molecular mass; this in turn will increase the amount of polymer chains surrounding the nanoparticle **[6, 7].** The higher polymer chains are, the more they inhibit the aggregation and/or the growth of the silver nanoparticles **[6]**. In addition, the increase of irradiation dose will increase the extent, rate of Ag^+ reduction and the nucleation rate which results in formation of metal nanoparticles **[8]**.

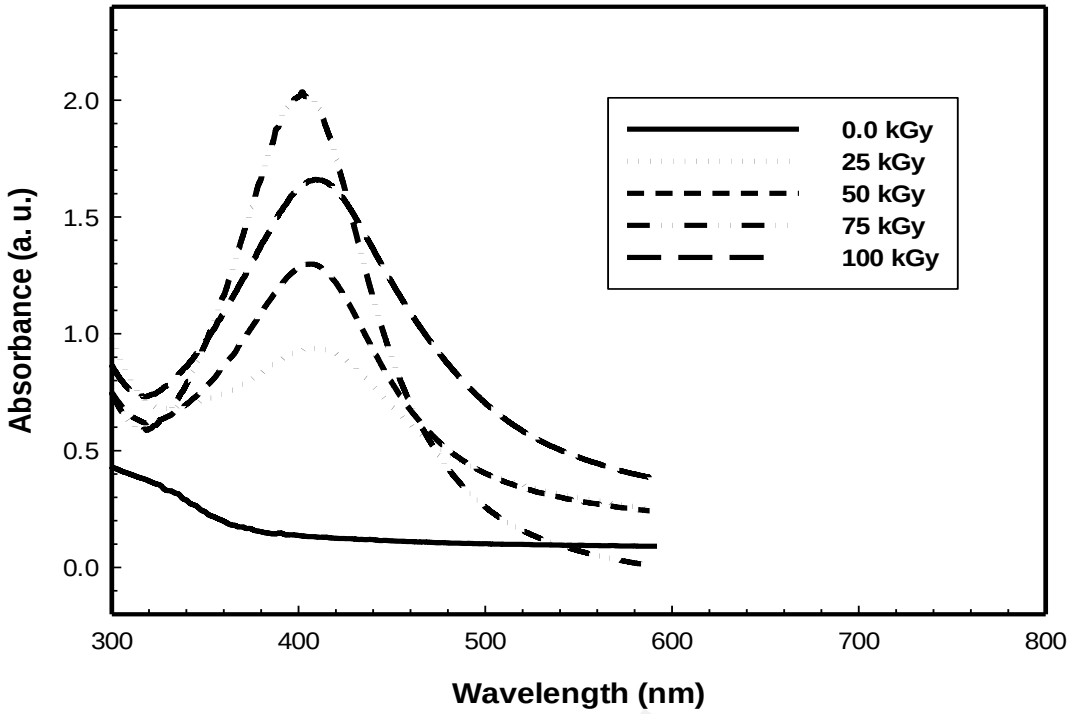

Fig.1. UV/VIS spectra of Ag/PVA nanocomposite films (0.005 M $AgNO_3$), gamma irradiated to various doses.

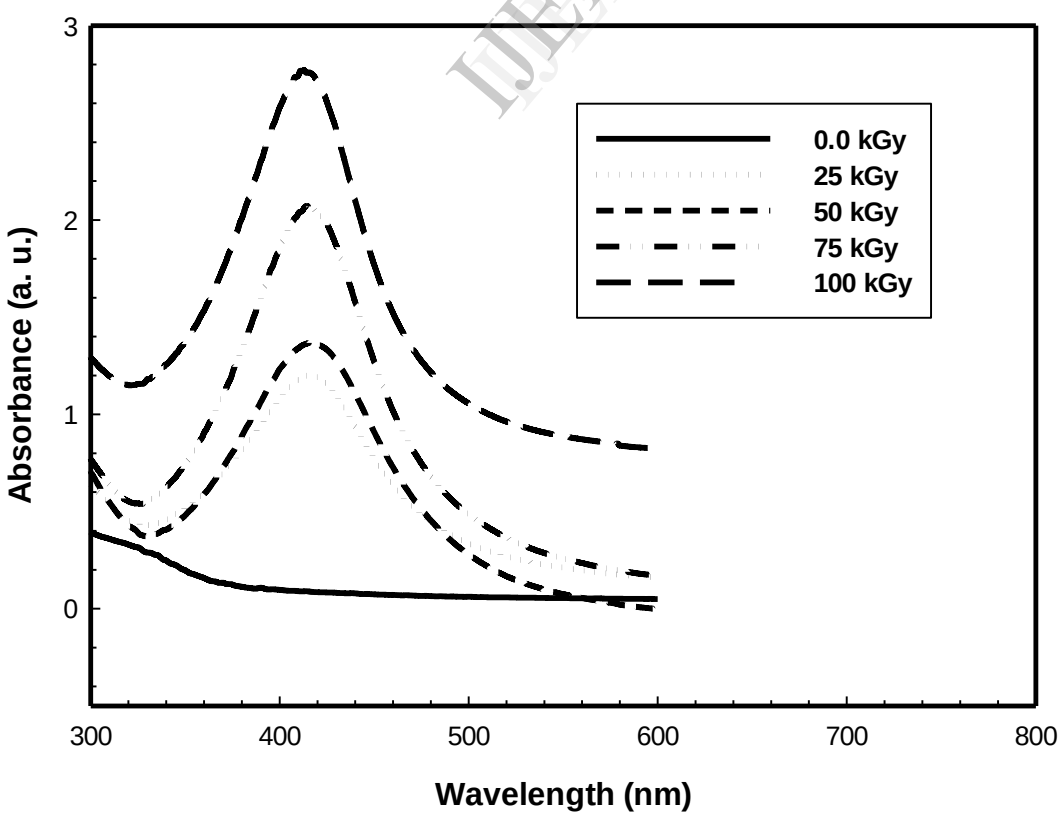

Fig. 2. UV/VIS spectra of Ag/PVA nanocomposite films (0.01 M $AgNO_3$), gamma irradiated to various doses.

Fig. 3 shows the UV/VIS spectra of irradiated Ag/PVA nanocomposite films containing different molar concentrations of $AgNO_3$. The characteristic peak of the Ag nanoparticles at 25 kGy for different molar concentration of $AgNO_3$ (0.005-0.1 M) appears in the range of 410 nm to 422 nm. These peaks are attributed to surface plasmon phenomenon, (i.e., cloud electromagnetic waves coupled with the conduction band (CB) electrons) **[9]**. With increasing the $AgNO_3$ molar concentration, the intensity of surface plasmon resonance peak gradually increased and slightly red shift was observed. Increasing the absorption intensity of surface plasmon resonance peak with increasing $AgNO_3$ molar concentration indicates a higher content of silver nanoparticles in the investigated Ag/PVA nanocomposite films. Higher concentration of Ag nanoparticles may lead to the red shift of surface plasmon resonance peak due to the multi poles interaction among the nanoparticles. In other words, the intensities of the SPR peak of the Ag nanoparticles increased with increasing Ag concentration, indicating that more silver nanoparticles were generated. The slight red shift of the peak maximum to longer wavelengths implies that the average sizes of the Ag nanoparticles slightly increased with increasing Ag^+ ion molar concentration. Also, one can deduce that the concentration of $AgNO_3$ may be decides the ultimately quantity of the metal nanoparticles in PVA matrix and also affect the size diameter, size distribution and type of nanoparticles.

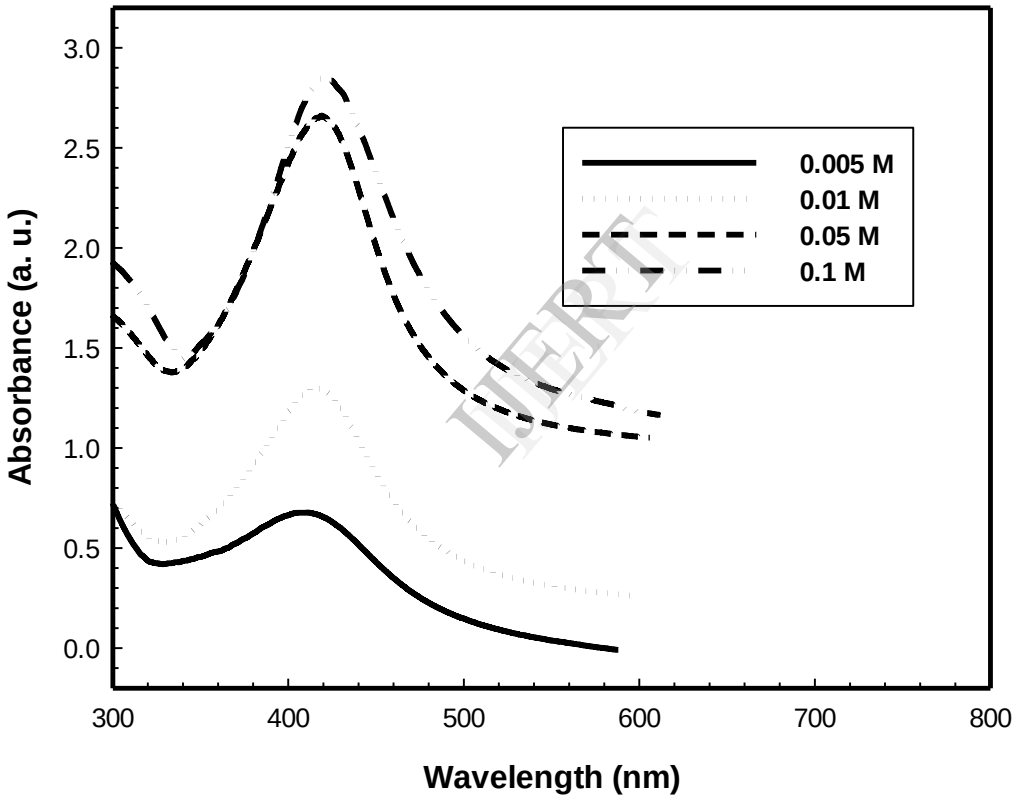

Fig. 3. UV/VIS spectra of Ag/PVA nanocomposite films containing different concentrations of $AgNO_3$ and gamma irradiated at the dose 25 kGy.

3.1.1. Estimation of particle size and optical band gap energy of Ag nanoparticles

The symmetry, sharpness and shape of the surface plasmon peak for the investigated samples are dependent factors for size determination of Ag nanoparticles. As shown above, the surface plasmon peaks of the investigated samples became more narrow and sharp with increasing either irradiation dose or $AgNO_3$ molar concentration. The symmetric and narrow absorption peak implies the narrow size distribution of the silver nanoparticles at higher $AgNO_3$ molar concentration and irradiation dose**.** Moreover, almost symmetric shape and narrow full width at half maximum (FWHM) of SPR peak indicates that the synthesized Ag nanoparticles are nearly spherical in shape. From the FWHM of SPR peak, the diameter (d, nm) of Ag nanoparticles have been estimated by assuming free particles behavior of conduction electron, using the following relation:

$$d = \frac{2h\upsilon f}{FWHM} \qquad (1)$$

where, υ_f is the Fermi velocity of electrons in bulk Ag (1.39×10^6 m/s) and h is the Plank's constant (6.626×10^{-34} J.S) **[10].** The average diameter of Ag nanoparticles was found to be in the range 30 to 15 nm as shown in **Table 1**. The obtained data of Ag nanoparticles diameter indicated that the Ag nanoparticles size decreases with either increase of irradiation dose or $AgNO_3$ molar concentration.

Table 1 Determination of the particle size from UV/Vis spectroscopic analysis

$AgNO_3$ conc. (M)	Irradiation dose (kGy)	Particle size (d, nm)
0.005	25	30.6
	50	26.5
	75	25.9
	100	21.7
0.01	25	27.3
	50	25.0
	75	24.4
	100	23.8
0.05	25	30.6
	50	28.0
	75	27.4
	100	26.9
0.1	25	26.7
	50	24.8
	75	21.2
	100	15.4

Due to the importance of optical band gap energy (E_g, eV) in the technology of nanomaterials, the value E_g was calculated from UV/VIS spectra for all investigated Ag/PVA nanocomposites according to Tauc's expression **[2]**.

$$(\alpha h\upsilon) = \beta(h\upsilon - E_g)^n \qquad (2)$$

where, **α** is the absorption coefficient corresponding to the fundamental absorption edge, **hυ** is the photon energy (eV), **β** is the constant known as the disorder parameter which is nearly independent of the photon energy and n represents the nature of the transition parameter which may have different values such as 1/2, 2, 3/2 or 3 for allowed direct, allowed indirect, forbidden direct and forbidden indirect transitions, respectively. The optical band gap energy was determined by plotting absorption coefficient α (υ) as $\{(\alpha h\upsilon)^2, (eV/cm)^2\}$ versus the photon energy (hυ, eV) as shown in **Fig.4**. The band gap energy was determined from the extrapolation of the linear section of the curves to the x-axis, in which $(\alpha h\upsilon)^2$ equals zero. The estimated optical band gap energies of the investigated samples are presented in **Table 2**. It can be seen that the optical band gap energy decreases with increasing the $AgNO_3$ molar concentration from 0.005 M up to 0.1 M for all gamma-irradiated samples. In addition, the results showed a strong dependence on the concentration of the $AgNO_3$ dopant showing a minimum value of band gap energy for the sample doped with a concentration of 0.1 M. On the other hand, it is clear from the result that the optical band energy showed a conflict behavior (slightly decrease or increase) as the irradiation dose was increased. The decrease in the band gap energy as irradiation dose was increased is attributed to further reduction of $AgNO_3$ to Ag nanoparticles. The increase in the optical band energy as the irradiation dose was increased may be due to agglomeration of Ag nanoparticles into the crosslinked network of PVA matrix. From **Table 2**, it can be seen that the factors influencing the values of E_g are the concentration of $AgNO_3$, irradiation dose and the structure and content of surrounding PVA nanoparticles.

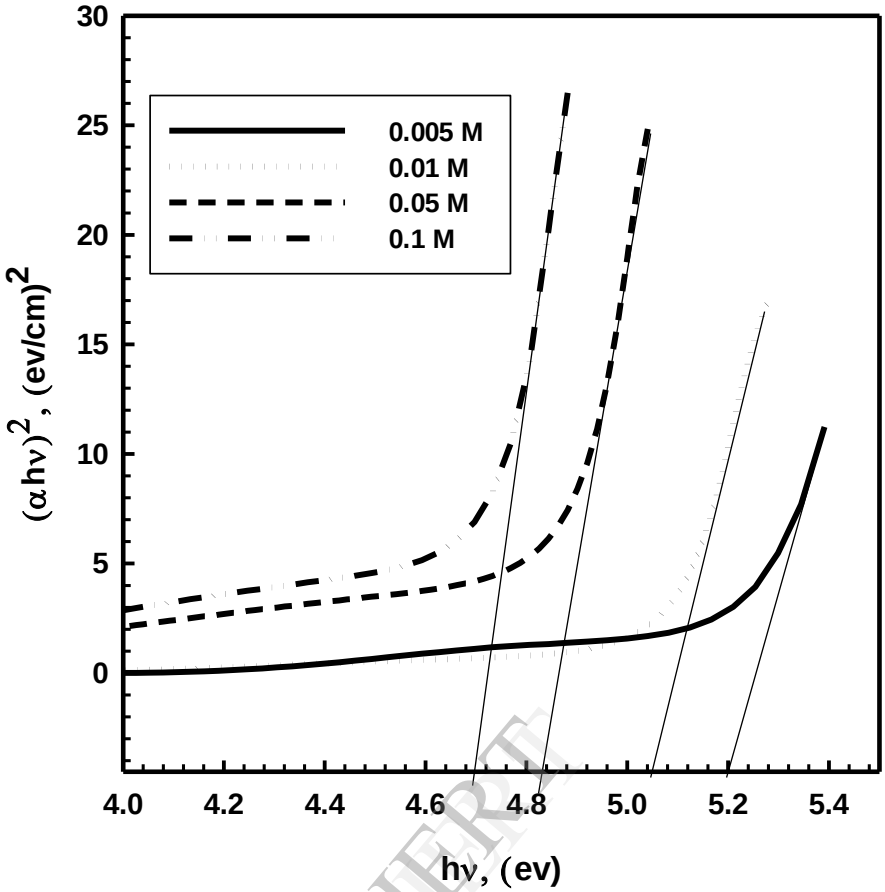

Fig. 4. Plots of $(\alpha h\nu)^2$ versus $h\nu$ for Ag/PVA nanocomposite films containing different molar concentrations of $AgNO_3$, gamma irradiated at the dose 25 kGy.

Table 2 The optical band gap (E_g, ev) energies for irradiated Ag/PVA nanocomposite films at different $AgNO_3$ molarconcentrations.

$AgNO_3$ conc., (M)	**E_g (ev)**			
	25 kGy	**50 kGy**	**75 kGy**	**100 kGy)**
Pure PVA	5.50	5.45	5.40	5.40
0.005	5.17	5.30	5.25	5.16
0.01	5.00	5.00	5.00	5.00
0.05	4.82	4.85	4.88	4.88
0.1	4.68	4.68	4.73	4.70

3.2. X-Ray diffraction characterization

Fig. 5 shows the XRD patterns of unirradiated pure PVA and irradiated Ag/PVA nanocomposites containing various molar concentrations of $AgNO_3$. The XRD pattern of unirradiated pure PVA exhibits strong and broad diffraction peak located at $2\theta = 19.66^o$ with a shoulder at $2\theta = 22.76^o$. The diffraction peak at $2\theta = 19.66^o$ corresponds to the (110) reflection, a plane which contains the extended planar zigzag chain direction of the crystallites. The shoulder peak at $2\theta = 22.76^o$ is related to the reflection from the plane (200). These peaks have resulted from the part crystallinity in PVA matrix. This crystallinity is a result of strong intermolecular and intramolecular hydrogen bonding between the PVA molecular chains **[11].**

The examination and comparison of diffraction patterns of irradiated Ag/PVA nanocomposites with that of unirradiated pure PVA lead to three remarks:

First, the irradiated Ag/PVA nanocomposites show four new diffraction peaks at 2θ = 37.8, 43.96, 64.34 and 77.48°. These discernible peaks can be indexed to the planes (111), (200), (220) and (311); respectively revealing that the Ag nanoparticles are formed in the PVA matrix and their crystal structure is face center cubic (FCC) structure according to JCPDS (No.4-0783). This is a confirmation of spontaneous reduction of Ag^+ ion to Ag^o nanoparticles in the metallic form using PVA chains and/or irradiation. Second, as the irradiation dose was increased from 25 to 75 kGy, the intensity of the Ag lines decreases and broadens gradually in accordance with their small grain sizes. Also, it can be seen that the prepared growth plane of the Ag nanoparticles is the (111) lattice plane which show the highest intensity all over the diffraction pattern. Secondary peaks at (200) and (220) reflection planes, corresponding to the high angle XRD pattern, supports the presence of Ag nanoparticles in nanocomposites. At higher irradiation dose (100 kGy), the Ag lines were intensified again due to the particles growth. Third, XRD patterns showed that the peak at 2θ = 19.66° shifts to the lower angle side from unirradiated pure PVA to irradiated Ag/PVA nanocomposite samples as shown in **Table 3**. The intensity of the PVA line at 2θ = 19.66° was decreased with increasing irradiation dose, indicating that the crystallinity is slightly deteriorated. This finding may reflect the fact that the polymer matrix in the Ag/PVA nanocomposite suffer from some kind of structural rearrangement due to irradiation.

Fig. 6 shows the XRD pattern of unirradiated PVA and irradiated Ag/PVA nanocomposite films containing different $AgNO_3$ molar concentration. It can be seen that the Ag peaks get sharper and narrower with increasing $AgNO_3$ molar concentration. This means that the increase of $AgNO_3$ molar concentration assist the growth of the Ag nanoparticles within the PVA matrix. In addition, the intensity of the observed peaks increases as a result of increasing $AgNO_3$ molar concentration up to 0.05 M and thereafter the intensity decreases for the nanocomposite containing 0.1 M. It can be clearly seen that the peak at 19.66° was broadened with increasing $AgNO_3$ molar concentration. The increase of broadening level with increasing $AgNO_3$ molar concentration can be attributed to the increase of Ag nanoparticle content. This broadening of the peak could also arise due to the micro-strain of the crystal structure arising from defects like dislocation and twining, etc. The defects are believed to be associated with the synthesized Ag nanoparticles as they grow spontaneously during the reaction **[12]**. The behavior of this peak is an indication of decreasing crystallinity of PVA matrix due to the presence of Ag nanoparticles. This finding can be correlated to the interaction and/or coordination between PVA and Ag nanoparticles which led to decrease of the intermolecular interaction between the PVA chains and thus the crystallinity. The way by which $AgNO_3$ and inconsequence the as-prepared Ag nanoparticles can affect the crystallinity of PVA may be proposed to occur by forming weak bonds with the polymer leading to what is referred to as quasi-crosslinking effect. These effects will eventually break the polymer chains and formation of some clusters with Ag nanoparticles. The weak crosslinks between the Ag surface and the polymer led to forming of smaller crystallites which in turn act to prevent ordering locally.

It is well known that the resulting diffraction pattern of a crystal is a fundamental physical property of the material. Analysis of the position and shape of the diffraction peaks lead to a knowledge of the inter planner spacing (d), lattice constant (a) and the average particle size (D), of the Ag nanoparticle. The d spacing is usually calculated using Bragg's equation **[13].**

$$n\lambda = 2\,d\sin\theta \qquad (3)$$

where, **λ** is the x-ray wavelength (λ = 0.154 nm), **n** is an integer number and equal to 1, 2, 3, etc, and **θ** is the angle of deviation of the diffraction beam. The average grain size of spherical crystallites can be determined by measuring the full wavelength at half maximum (FWHM) of the diffraction peaks at 2θ = 37.8°, (111) reflection. The particle size 'D' was calculated based on the regular broadening of XRD peaks as a function of decreasing crystallite size. This broadening is a fundamental property of XRD described by well-established Scherer theory **[14]**:

$$D = \frac{K\lambda}{\beta Cos\theta} \qquad (4)$$

where, D is the particle diameter (nm), K is a constant equals 0.9, λ is the X-ray wavelength; (Cu Kα = 1.540˚ A), β is FWHM of the peak corresponding to plane (111 reflection) and θ is the diffraction angle obtained from 2θ values corresponding to maximum intensity peak in XRD pattern. The calculated values of crystalline particle size (D, nm) are listed in **Table 3**. The careful analysis for the position and the shape of the (111) reflection peak illustrates that there is a gradual shift towards lower angle with increasing irradiation dose and towards higher angle with increasing $AgNO_3$ molar concentration. The shift towards higher angle as a result of increasing $AgNO_3$ molar concentration corresponds to a contraction in the d-spacing values. The d-spacing contraction is expected to occur due to the high-to-surface volume ratio **[15]**. From **Table 3**, it can be clearly seen that both $AgNO_3$ and irradiation dose are determining factors in controlling the particle size of Ag nanoparticles in PVA matrix. It can be seen that with increasing irradiation dose up to 75 kGy, the particle size decreased and then increased at 100 kGy. Also, the particle size increases gradually with increasing $AgNO_3$ molar concentration up to 0.05 M and thereafter it decreased at higher $AgNO_3$ molar concentration (0.1 M). These results are in a good agreement with UV/VIS data.

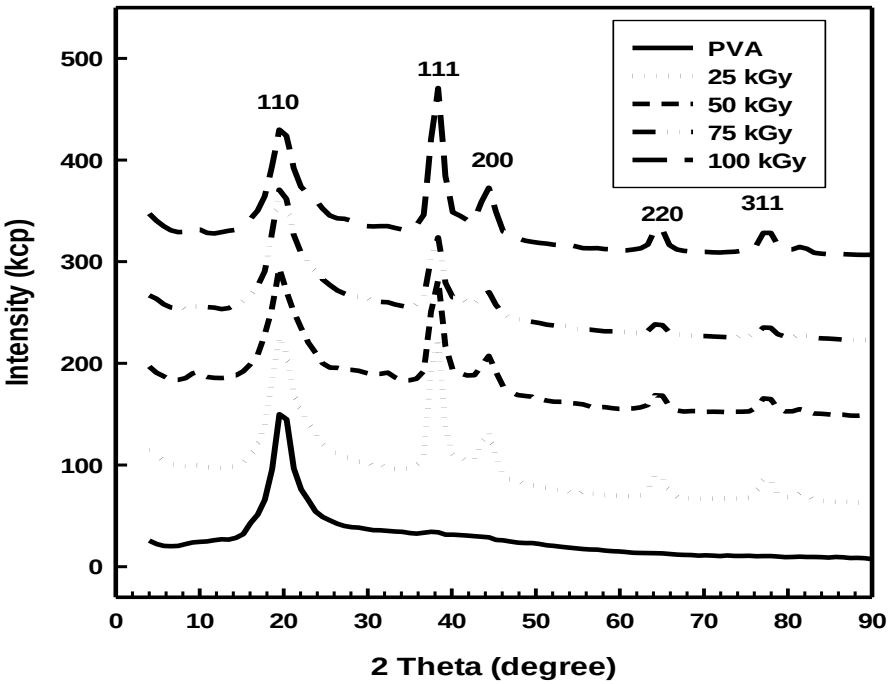

Fig. 5. XRD patterns of unirradiated PVA and Ag/PVA nanocomposite films (0.05 M $AgNO_3$), gamma irradiated at various irradiation doses.

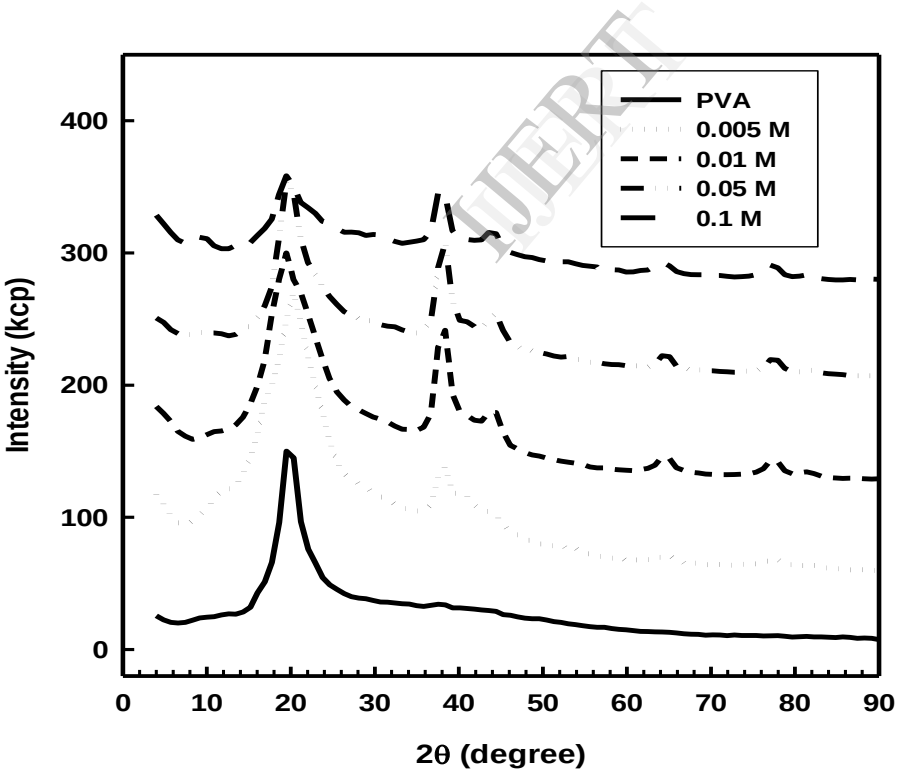

Fig. 6. XRD patterns of unirradiated PVA and PVA/Ag nanocomposite films containing different concentrations of $AgNO_3$ and gamma irradiated at the dose 75 kGy.

Table 3: The XRD parameters of Ag/PVA nanocomposite films

$AgNO_3$ conc.,(M)	**Dose, (kGy)**	**2θ (degree)**	size (nm)
		Ag (37.8^o)	
0.005	25 50 75 100	38.16 38.12 38.10 38.09	16.2 16.0 15.7 15.9
0.01	25 50 75 100	38.16 38.14 38.20 38.11	17.5 17.2 17.0 16.5
0.05	25 50 75 100	38.22 38.18 38.17 38.15	24.8 22.7 19.4 22.7
0.1	25 50 75 100	38.73 38.68 37.88 37.80	20.7 20.2 20.0 19.0

3.3. Catalytic evaluation of Ag nanoparticles with Ag/PVA nanocomposite

For the investigation of the reduction of 4-nitrophenol (4-NP) to 4-aminophenol (4-AP), the UV/VIS spectrum of 4-NP aqueous solution was carried out in the presence of $NaBH_4$ as a reducing agent and in the absence of Ag nanoparticles. It was found that the absorbance value and the peak position of 4-NP solution (at $\lambda_{max} \approx 400$ nm) remained the same even after a couple of days, suggesting that the reduction reaction did not proceed in the absence of Ag nanoparticles. The addition and mixing of the Ag/PVA nanocomposite film to the reaction mixture caused a successive decrease in the intensity of the peak of the nitro compound (at $\lambda_{max} \approx 400$ nm) and the formation of a new absorption band (around $\lambda_{max} = 300$ nm), which is attributed to the formation of 4-AP as shown in **Fig. 7**. Although, it may be accepted that the absorbance band at $\lambda_{max} = 300$ nm signifies the formation of 4-AP, this can also be visualized with the discoloration of the characteristic yellow color of 4-NP solution. After the yellow color is completely discharged, i.e. after complete reduction reaction of 4-NP to 4-AP, the peak due to the nitro compound at $\lambda_{max} = 400$ nm was no longer observed. It should be noted that the mechanism of this reduction reaction probably involves more complicated intermediates present on the surface of the Ag nanoparticles and hence remains a point of debate. However, the isosbestic point at approximately $\lambda_{max} = 325$ nm, indicates a clean conversion of 4-NP to 4-AP without side reactions. The reduction conversion of 4-NP with borohydride catalyzed by Ag nanoparticles to 4-AP is of industrial and environmental importance. Metal nanoparticles have high Fermi potential, and nanometer size regime which leads to the lowering of reduction potential value, and hence metal nanoparticles can function as a catalyst for many electron-transfer reactions **[16]**.

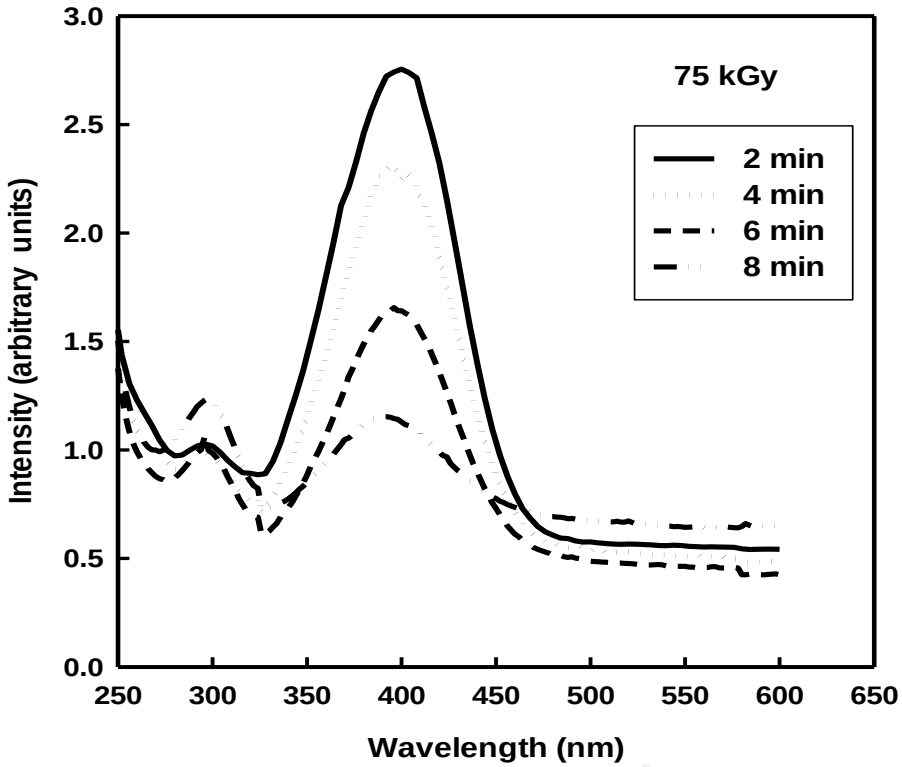

Fig. 7. UV/VIS spectra of the reduction of 4-NP by the catalyzed reduction with 75 kGy irradiated Ag/PVA (0.05 M) catalysts at 2 min interval

Actually $NaBH_4$ served here as the reducing agent for nitro compounds to produce the corresponding amino compounds. A little $NaBH_4$ is always decomposed in the reaction medium during the course of reaction. So an excess amount of $NaBH_4$ was always employed. As soon as $NaBH_4$ was added, the silver nanoparticles started the catalytic reaction by relaying electrons from the donor BH_4^- to the substrate 4-NP (acceptor) only after the adsorption of both onto the particle surfaces as shown schematically in **Fig. 8**. Here, as the catalyst particles are held on the solid surfaces, there was no chance of agglomeration of silver nanoparticles due to the presence of larger amounts of $NaBH_4$ **[17]**.

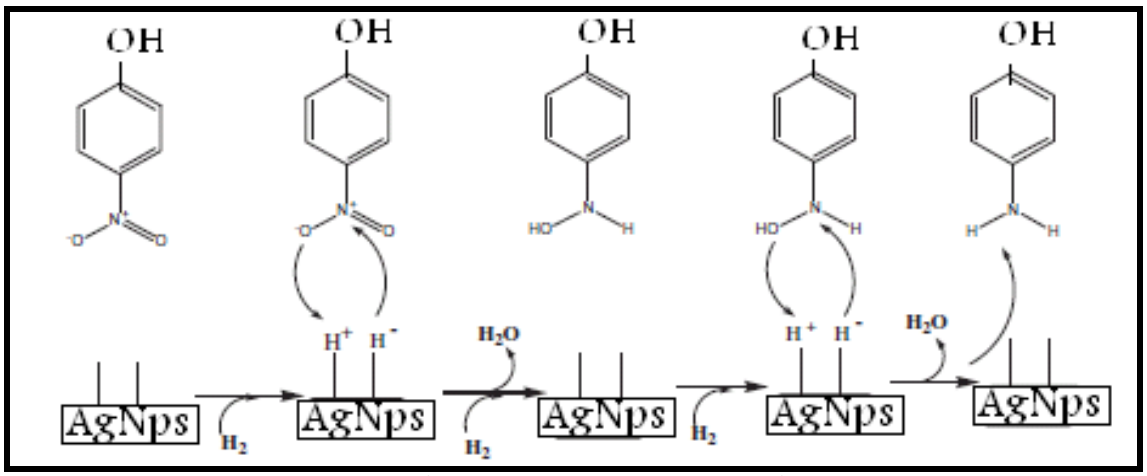

Fig. 8. Proposed mechanism for the AgNPs catalyzed hydrogenation of 4-nitrophenol (4-NP).

Considering the absorbance versus time plots, the reaction kinetics can be described as $\ln(A/A_o) = kt$, where k is the apparent first order rate constant (min^{-1}), t is the reaction time (min), A and A_o are the absorbance corresponding to the concentration of 4-NP at time t and zero time, respectively. **Fig. 9** shows a linear relationship between $\ln(A/A_o)$ and reaction time t in the reduction catalyzed by Ag nanoparticles. The rate constant k was calculated to be 0.1 min^{-1}. The data revealed that the first order rate constant increased with increasing the amount of Ag nanoparticles.

In conclusion, a new simple method of making silver nanoparticles catalysts supported on PVA polymer matrix has presented. The Ag/PVA catalyst was found to be active for the reduction of aromatic nitro compounds to the corresponding

amino derivatives. Furthermore, the procedure is simple and useful for large scale synthesis. This method may be useful in developing the process for the conversion of 4-NP to 4-AP in aqueous solution under mild condition.

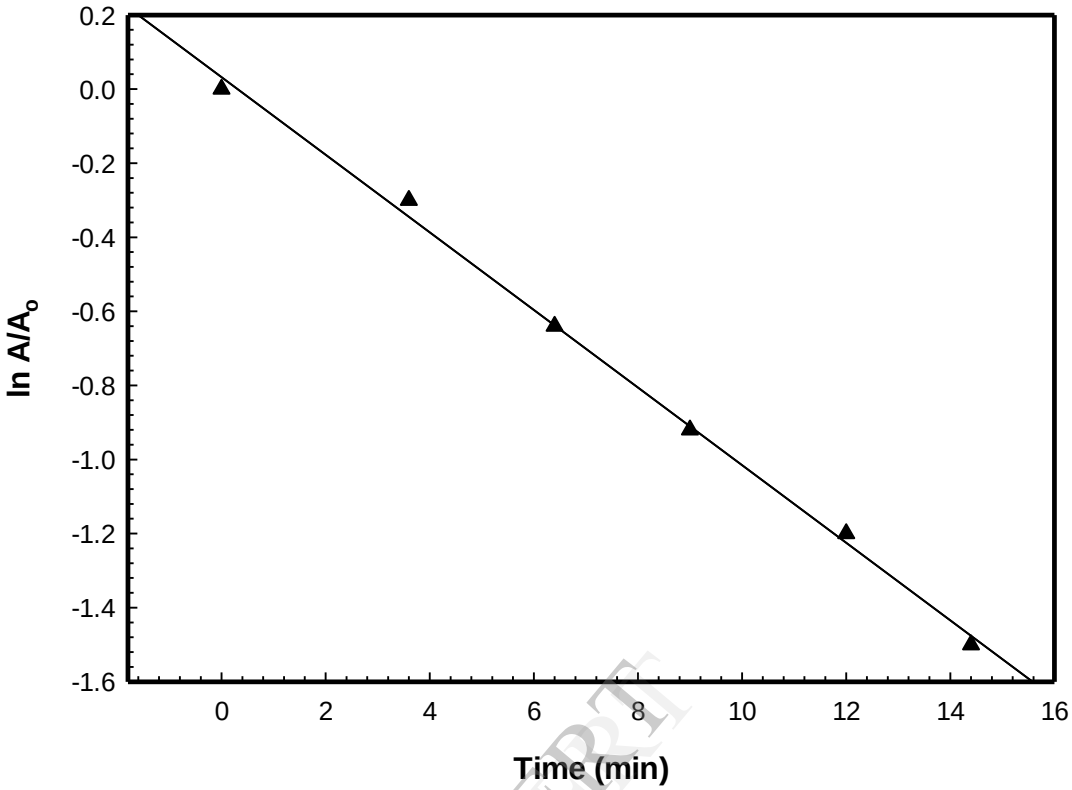

Fig. 9. Plot of ln(A/A$_o$) verses time corresponding to the reduction of 4-nitrophenol by Ag/PVA nanocomposites at 298 K.

V. CONCLUSION

Ag/PVA nanocomposites were prepared successfully using γ-irradiation method. Our synthetic route did not need complicated apparatus, expensive surfactants or additional reducing agents. The obtained data regarding the change of the absorption intensity and wavelength at maximum absorption and the size of Ag nanoparticles as a function of either irradiation dose or Ag^+ ion molar concentration pointed the following remarks: The intensity of the absorption bands, which is proportional to the number of silver nanoparticles, goes higher, indicates that more reduction of Ag^+ to Ag nanoparticle as the irradiation dose increases. The intensity of absorption spectra goes higher but there was a slight shift to higher wavelength (red shift) with increasing the concentration of $AgNO_3$. The band gap energy decreases following the $AgNO_3$ molar concentration from 0.005 M up to 0.1 M for all γ-irradiated samples. On the other hand, the band gap energy showed a conflict behavior (slightly decrease or increase) as the irradiation dose increased. The XRD pattern of pure PVA exhibits strong and broad diffraction peak located at $2\theta = 19.66^o$ which is due to crystallinity part, where the irradiated Ag/PVA nanocomposite samples show four new diffraction peaks at $2\theta = 37.8, 43.96, 64.34$ and 77.48^o, revealed that the Ag nanoparticles are formed in the PVA matrix. The calculated values of crystalline particle size (D, nm) showed that both $AgNO_3$ and irradiation dose are determining factors in controlling the particle size of Ag nanoparticles in PVA matrix. Catalytic evaluation of Ag/PVA nanocomposite films in the reduction of 4-Nitro phenol (4-NP) showed that, in the absence of any catalyst (Ag/PVA film), the absorbance value and the peak position of 4-NP (at $\lambda_{max} = 400$) remained the same even for a couple of days. Addition and proper mixing of the Ag/PVA catalyst to the reaction mixture caused the successive decrease in the intensity of the peak of the nitro compound (at $\lambda_{max} \approx 400$ nm) and the formation of a new absorption band around $\lambda_{max} \approx 300$ nm, which is attributed to the formation of 4-AP. These indicate that Ag/PVA nanocomposite films successive catalyst for a reduction of 4-nitrophenol.

REFERENCES

1- P.K. Khanna, Narendra Singh, Shobhit Charan, V.S Subbarao, R. Gokhale, and U.P Mulik. Synthesis and characterization of Ag/PVA nanocomposite by chemical reduction method. Materials Chemistry and Physics. 93 (2005) 117-121.
2- Z. Jovanovic, A. Radosavljevic, M. Siljegovic, N. S. Stankovic, Z. K Popovic. Structural and optical characteristics of silver / poly (N-vinyl-2-pyrrolidone) nanosystems synthesized by g-irradiation. Radiation Physics and Chemistry 81(2012) 1720.
3- W. E Hutter., and J. H. Fendler. Exploitation of localized surface plasmon resonance, Advanced Materials. 19 (2001) 1685-1706.
4- S.S. Gasaymeh, S. Radiman, L. Y. Heng, E. Saion, and G. M. Moahmed Saeed. synthesis and characterization of silver/polyvinyl pyrrolidone (Ag/PVP) nanoparticles using gamma irradiation technique. African physical review. (2010) 4:0006.

5- S. Weihong, Z. Xiaoxiao, Y. Hongzong, S. Panpan, and L. Xiaoyan. Preparation and Storage of Silver Nanoparticles in Aqueons Polymers Chin. Chem. 27 (2009) 717-721.
6- Y. Liu, S. Chen, L. Zhong, and G. Wu. Preparation of high-stable silver nanoparticle dispersion by using sodium alginate as a stabilizer under gamma radiation Radiat. Phys. Chem. 78 (2009) 251-255.
7- I. V. Ravindrachary, R. F. Bhajantri, S. D. Praveena, B. Poojary, D. Dutta, and P. K. Pujari. Optical and microstructural studies on electron irradiated PMMA: A positron annihilation study Polym. Degrad. Stab. 95 (2010) 1083-1091.
8- C. Kan, C. Wang, and L. Zhu. Formation of gold and silver nanostructures within polyvinylpyrollidone (PVP) gel. Solid State Chem. 183 (2010) 858-865.
9- M. A. A. Omar, E. Saion, M. E. M. Gar-elnabi, E. A. A. Balla, M. Dahlan Kh. and Y. M. Yousif. Gamma radiation synthesis ang characterization of polyvinyl alcohol/silver nanocomposites film. J.sc. tech. 12 (2011) 3212.
10- S. Mahendia, A. K. Tomar, and S. Kumar. Electrical conductivity and dielectric spectroscopyic studies of PVA-Ag nanocomposite films. Journal of alloys and compounds. 508 (2010) 406-411.
11- H. E. Wael, K. A. Yasser, S. Yasser, A. A. Atef, and M. Amira. Gamma-irradiation assisted seeded growth of Ag nanoparticles within PVA Matrix. Materials Chemistry and Physics. 128 (2011) 109.
12- H.C. Warad, S.C. Ghosh, B. Hemtanon, C. Thanachayanont, and J. Datta. Luminescent nanoparticles of Mn doped ZnS passivated with sodium hexametaphosphate Sci. Tech. Advan. Mater. 6 (2005) 296.
13- T. Thongtem, A. Phuruangrat, and S. Thongtem. Preparation, characterization and photoluminescence of nanocrystalline calcium molybdate. Journal of Alloys and Compounds. 481(2009) 568.
14- S. H. Wang, W. Xu, H. Si, X. Tao, S. Lou, Z. Du, and L.S. Li. Synthesis and assembly of monodisperse spherical Cu_2S nanocrystals Colloid Interface Sci. 330 (2009) 483.
15- K. K. Nada, S. N. Sarangi, and S. N. Sahu. CdS Nanocrystalline films: Composition, surface, crystalline size, structural and optical absorption studies Nanostructured mater. 10 (1998) 1401.
16- M. Nemanashi, R. Meijboom. J. Colloid. Interf. Sci., 2013, 389, 260.
17- P. Liu and M. Zhao. Silver nanoparticle supported on halloysite nanotubes catalyzed reduction of 4-nitrophenol (4-NP). Applied Surface Science. 255 (2009) 3989-3993.